

Effects of exosomes derived from the induced pluripotent stem cells on skin wound healing

Hitoshi Kobayashi¹, Katsumi Ebisawa¹, Miki Kambe¹, Takatoshi Kasai², Hidetaka Suga², Kae Nakamura³, Yuji Narita⁴, Aika Ogata⁴, and Yuzuru Kamei¹

¹Department of Plastic and Reconstructive Surgery, Nagoya University Graduate School of Medicine, Nagoya, Japan

²Department of Endocrinology and Diabetes, Nagoya University Graduate School of Medicine, Nagoya, Japan

³Department of Obstetrics and Gynecology, Nagoya University Graduate School of Medicine, Nagoya, Japan

⁴Department of Cardiac Surgery, Nagoya University Graduate School of Medicine, Nagoya, Japan

ABSTRACT

Recently, the effects of stem cell supernatants or exosomes, such as skin wounds, have attracted attention. However, the effects of the induced pluripotent stem (iPS) cell-derived exosomes (iPS-Exos) have not been investigated in detail. Here, we investigated the effects of iPS-Exos on skin wound healing using an animal model. We isolated iPS-Exos from the iPS cell culture media. Control exosomes were isolated from unused iPS cell culture media (M-Exos). We first observed the morphologic characteristics of the isolated exosomes and examined the expression of surface antigens. The effects of these exosomes on the migratory response and proliferation of fibroblasts were analyzed as well. Additionally, using a diabetic ulcer model, the effects of iPS-Exos and M-Exos on skin wound healing were investigated. Transmission electron microscope analysis demonstrated that the size of iPS-Exos (120 ± 25 nm) was significantly larger than that of M-Exos (≤ 100 nm). Flow cytometry analyses showed that iPS-Exos were positive for CD9, CD63, and CD81, whereas they were negative for HLA-ABC and -DR expression. The migratory ability of fibroblasts cocultured with iPS-Exos was shown to be higher than that of the cells cocultured with M-Exos, as demonstrated using scratch assay. Skin wound healing model results showed that the administration of iPS-Exos results in a faster wound closure compared with that observed in the M-Exo group. In conclusion, the results obtained here indicate that iPS-Exos may promote the migration of fibroblasts *in vitro* and *in vivo*, suggesting the possibility of using iPS-Exos for the treatment of diabetic ulcer.

Keywords: exosome, induced pluripotent stem cell, wound healing, diabetic ulcer

This is an Open Access article distributed under the Creative Commons Attribution-NonCommercial-NoDerivatives 4.0 International License. To view the details of this license, please visit (<http://creativecommons.org/licenses/by-nc-nd/4.0/>).

INTRODUCTION

According to the estimates provided in the Diabetes Atlas by the International Diabetes Federation (IDF), approximately 415 million people suffer from diabetes worldwide.¹⁾ The increasing number of diabetic patients has raised a number of economic issues and medical challenges,

Received: September 12, 2017; accepted: November 14, 2017

Corresponding author: Hitoshi Kobayashi, DDS, PhD

Department of Plastic and Reconstructive Surgery, Nagoya University Graduate School of Medicine 65

Tsurumai-Cho, Showa-Ku, Nagoya 466-8550, Japan

Phone: +81-52-741-2111, Fax: +81-52-744-2260, Email: fmwxq374@ybb.ne.jp

because the disease is associated with various difficult-to-treat complications.²⁻⁵⁾ Therefore, the development of effective treatments for these complications is required in order to improve the quality of life of diabetic patients.

Diabetic foot crush, one of the potential diabetes-related complications, develops in approximately 25% of diabetic patients. Skin injuries, associated with the peripheral nervous system dysfunction, are usually observed during the development of this condition, and it is accompanied by the peripheral arterial obstructive disease and delayed wound healing. These patients also show an increase in infectious disease predisposition, due to their impaired immune system.⁶⁾ Therapeutic options include the control of blood glucose levels and wound management, but the beneficial effects remain limited.

In recent years, a number of studies aimed at the development of cell therapies for the treatment of various diseases, including diabetic foot ulcer, have been conducted. These include the application and transplantations of platelets, progenitor cells, and various types of stem cells, including somatic stem cells and embryonic stem (ES)/induced pluripotent stem (iPS) cells.⁷⁾ However, these cell therapies were shown to induce some serious adverse effects, such as the development of pulmonary infarctions and tumor formation. These risks may be avoided by using cultured cell supernatants, which have been proven to be effective for the treatment of skin wounds.⁸⁻¹⁰⁾ The results of these studies indicated that exosomes, microvesicles found in the culture media, may play an important role in the healing of skin wounds. Exosome is a microvesicle with a diameter of 50–200 nm, which is exocytosed with the lipid bilayer composed of phospholipids and surface antigens unique to the exosomes.¹¹⁻¹⁴⁾ It was reported that miRNA and proteins found in the exosomes may mediate the therapeutic effects by transmitting genetic and non-genetic information between cells.

To date, the effects of iPS cell-derived exosomes (iPS-Exos) on skin wound healing have not been investigated. In this study, we evaluated the effects of iPS cell-derived exosomes on the migration and proliferation of fibroblasts in culture and skin wound healing using a diabetic mouse model.

MATERIALS AND METHODS

Preparation of iPS Cell-Derived Exosomes

Here, we used iPS cell line (201B7) provided by the RIKEN institute (Saitama, Japan), cultured in Dulbecco's Modified Eagle Medium (DMEM)-F12 supplemented with non-essential amino acids, 200 mM L-glutamine, KnockOut Serum Replacement (KSR), and 0.1 M 2-mercaptoethanol. Cells were passaged when the confluence reached 80%, and the conditioned media (CM) were collected 2–3 days before passaging the cells, and used for the experiments. iPS-Exos were purified using MagCapture Exosome Isolation Kit PS (Wako, Osaka, Japan) and stored at –80°C. The iPS cell medium was incubated for the same time and exosomes (M-Exo) recovered by the same procedure were used as controls.

Electron Microscopy

Transmission electron microscope (TEM) JEM-1400 (Hitachi High-Technologies Corporation, Tokyo, Japan) was used to examine the morphology of iPS-Exos. Exosomes in 2 µl of phosphate-buffered saline (PBS) were placed on formvar carbon-coated copper electron microscopy grids and incubated for 1 min at 25°C. The grids were treated with 2% uranyl acetate for 10 s. The grid was allowed to semi-dry at room temperature before TEM imaging.

Flow Cytometry

The exosomes obtained from 80 ml CM were used for flow cytometry (FCM) analysis as previously described.¹⁵⁻¹⁷⁾ Exosomes isolated from the media were used as a control (M-Exos). Purified iPS-Exos were incubated with 10 µl aldehyde/sulfate latex 4-µm-beads (Invitrogen) for 15 min at room temperature, followed by the addition of PBS to a final volume of 400 µl, after which the samples were incubated in a test tube rotator wheel overnight at 4°C. Exosome-coated beads were incubated with 40 µl of 1 M glycine (Wako) for 30 min at room temperature to block any remaining binding sites. After the addition of 600 µl PBS, the beads were microcentrifuged for 3 min at 4000 rpm at room temperature, which was followed by the removal of supernatants. Beads were resuspended in 1 ml PBS/0.5% bovine serum albumin (BSA) and microcentrifuged for 3 min at 4000 rpm at room temperature. After washing the beads twice, we resuspended the beads in 100 µl PBS with 0.5% BSA and incubated 10 µl of the coated beads with 20 µl anti-exosomal protein antibody for 1 h at 4°C. The exosome-coated beads were incubated with phycoerythrin (PE)-conjugated CD63 or CD81 or isotype control antibody and fluorescein-5-isothiocyanate (FITC)-conjugated CD9, HLA-ABC, or HLA-DR, or the isotype control antibody (BD Biosciences Pharmingen) for 30 min at 4°C with gentle agitation. After washing in PBS/0.5% BSA, the samples were resuspended in 500 µl PBS/0.5% BSA and analyzed by FACSCalibur (Becton Dickinson and Company) with FlowJo software (TreeStar, Inc.).

Fibroblasts

Fibroblasts were isolated from 10-week-old male, pathogen-free, genetically diabetic C57BLKS/J-Leprdb (db/db) mice. db/db mice were obtained from Japan SLC (Hamamatsu, Japan). All animal protocols were approved by the Animal Care and Use Committee of Nagoya University Graduate School of Medicine. Mice were sacrificed, and the trunk skin was isolated by sharp dissection, while special care was taken to remove the underlying adipose tissue. The collected skin tissue was trimmed to 2 × 4 cm, which was followed by the isolation of fibroblasts using the Whole Skin Dissociation Kit (Miltenyi Biotec). The isolated fibroblasts were resuspended in DMEM containing 10% FBS and 1% antibiotic/antimycotic solution (100 µg/ml penicillin and 100 µg/ml streptomycin; Wako), and cultured in the atmosphere with 5% CO₂ at 37°C. The culture medium was replaced every 2 days. The cells were passaged before reaching confluence.

Scratch Assay

Scratch assay was performed as previously described.¹⁸⁾ Exosome-stimulated cell migration was investigated using the CellPlayer Cell Migration 96-well assay kit and monitored by the automated Incucyte ZOOM-HD-2CLR (Essen Bioscience, Welwyn Garden City, Hertfordshire, UK). Primary cultured fibroblasts (passage 1) were seeded in an Essen Imagelock 96-well plate at the density of 1 × 10⁵ cells/well and were maintained until reaching confluence. A wound was made in cell monolayer using a 96-well wound-maker tool with PTFE pin tips (Essen Bioscience) according to the manufacturer's instructions. Afterward, the media were removed from the samples, and the cells were washed twice in PBS to remove the dislodged cells. The scratched wells were then divided into one treatment arm (iPS-Exo) and one control arm (M-Exo). The plate was inserted into the Incucyte ZOOM-HD-2CLR and incubated in 5% CO₂ at 37°C. After 12 h of incubation, 0, 10, 50, 100, or 200 µg/ml of exosomes were added to the wells, images were captured at 1 h intervals, and data were analyzed by using the IncuCyte software (Essen Bioscience). Relative wound density (RWD), which measures the relative cell density in the wounded and non-wounded areas at each time point, was used to assess the rate of cell migration.

Proliferative Assay

The effects of iPS-Exo on the proliferation of fibroblasts were evaluated using the CellPlayer Cell Migration 96-well assay kit and Incucyte ZOOM-HD-2CLR. Fibroblasts were seeded at 4×10^3 cells/well in 96-microwell plate (Nunc). After 12 h of incubation, 100 µg/ml of exosomes were added to the wells, high-density phase-contrast images were acquired at 1-h intervals, and data were analyzed using the IncuCyte software tool.

Mouse Diabetic Model

Nine-week-old adult male, pathogen-free, genetically diabetic C57BLKS/J-Leprdb (db/db) mice, weighing 41.0–45.5 g, were obtained from Japan SLC. After 1 week of acclimatization, the animals were individually housed in animal care facility maintained at 24°C in 30% humidity with a 12-h light-dark cycle. Water and standard rodent laboratory chow were available *ad libitum*. All animal experiments were performed in accordance with the Guide for Animal Experimentation of Nagoya University School of Medicine.

Wound-Healing Mouse Model

The excisional wound-splinting model was generated as described previously.¹⁹⁾ Briefly, the animals were anesthetized, shaved, and two 8-mm full-thickness excisional skin wounds were created on each side of the midline. A donut-shaped silicone splint (Shinoda Gomu Co Ltd, Tokyo, Japan) was placed and affixed so that the wound was centered within the splint, and interrupted 5–0 nylon sutures (Alfresa Pharma Corp., Osaka, Japan) were made to stabilize its position (Fig. 1). Mice were randomly assigned to three different treatment groups, which were subcutaneously injected at wound sites with PBS, M-Exo, or iPS-Exo. The exosomes (4 µg/20 µl PBS) were injected into four sites around the wounds and the wound beds in the respective groups (Fig. 2). Tegaderm (3M, MN, USA) was used for to cover the wounds.

Wound Closure Analysis

On day 0, 1, 3, 5, 7, 10, 14, 18, 21, and 28 after making the wound, images of 10 independent fields of each wound were obtained using a digital camera of 12.9 megapixels (Canon Inc, Tokyo, Japan). Wound area was measured using the public domain software ImageJ ver.1.47 (NIH, MD, USA). Wound closure percentage was calculated as follows:

$$\text{Wound area (\%)} = \text{AW/IW} \times 100 \quad (\text{IW, initial wound area; AW, wound area at each time point})$$

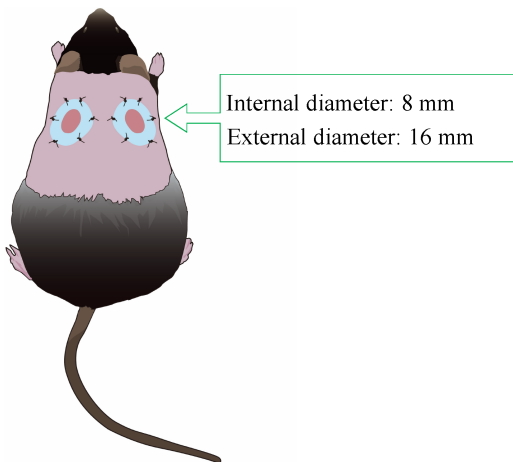
Histological Analysis

For histological analyses, skin samples excised from the wound sites were fixed in 4% paraformaldehyde, embedded in paraffin, and 4-µm thick sections were prepared, followed by hematoxylin and eosin (H&E) staining for histological observation.

Immunofluorescence Analysis

To examine angiogenesis induced by the exosomes in the wounded skin, the expression of CD31 and α-smooth muscle actin (SMA) was examined by immunofluorescence staining. Tissue sections were blocked in 10% donkey serum for 30 min at room temperature and incubated with rat anti-mouse CD31 (1:50; Dianova, Hamburg, Germany) and rabbit anti-α-SMA (1:500; Abcam, Cambridge, UK) antibodies overnight at 4°C. Tissue sections were stained with secondary Alexa-Fluor 594-conjugated donkey anti-rat (1:250; Thermo Fisher Scientific, Yokohama, Japan) and Alexa-Fluor 488-conjugated donkey anti-rabbit antibodies (1:250; Thermo Fisher Scientific), followed by counterstaining with 6-diamidino-2-phenylindole (DAPI). Images were acquired

Exosome roles in wound healing

**Fig. 1** Animal model

Excisional wounds were created bilaterally in the dorsal skin of diabetic mice, and silicone splint was placed and affixed. The stents prevented wound contraction.

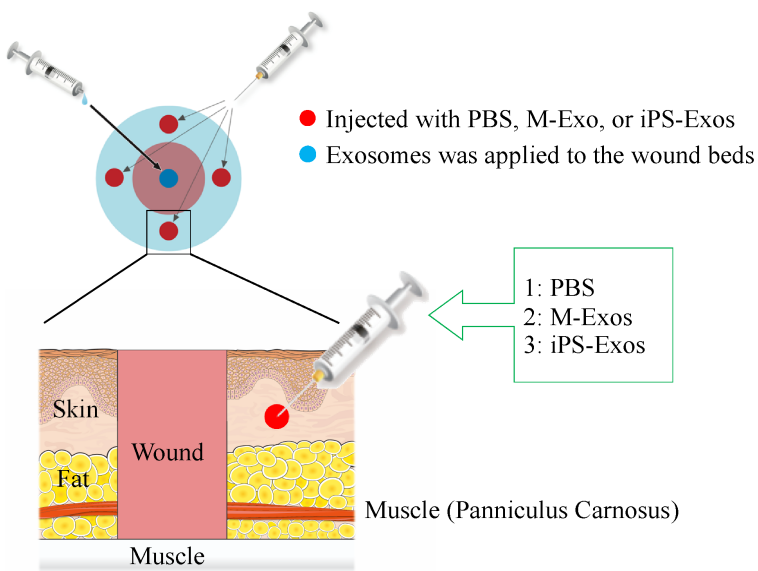


Fig. 2 Topical application of induced pluripotent stem cell-derived exosomes (iPS-Exos) to the wound beds
The wounds made in the dorsal skin areas were treated with phosphate buffered saline (PBS; untreated group), M-Exo (control group), or iPS-Exo (experimental group). iPS-Exo, M-Exo and PBS were injected at four sites into the subcutaneous layer around the wound.

with Olympus VS120 microscope. The newly-formed vessels were identified by CD31 staining, whereas mature vessels were identified as CD31 and α -SMA double-positive vascular structures. The number of newly-formed vessels and mature vessels was determined in three random fields per each section using the ImageJ software. To identify neurofilaments, we stained the sections with polyclonal rabbit NF200 antibody (1:500; Abcam). Using BIORÉVO VS120 fluorescence

microscope (Olympus, Tokyo, Japan), we quantified NF200-positive neurofilaments in each wound area, in order to determine nerve density (number of neurofilaments/mm²). In all experiments, a blinded investigator recorded the findings.

Statistical Analysis

The obtained results were expressed as mean \pm standard error of mean (SEM) and analyzed using one-way analysis of variance (ANOVA). Statistical significance was determined using GraphPad Prism software, version 5.0 (GraphPad Software, CA, USA) and P values < 0.05 were considered statistically significant. Comparisons of results obtained in proliferative assay between the groups was performed using Student's *t*-test. Statistical analyses were performed using the JMP statistical package, version 10.0.2 (SAS Institute, NC, USA) and P values < 0.05 were considered statistically significant.

RESULTS

Characterization of iPS-Exos

TEM analyses of iPS-Exos demonstrated that these vesicles have spheroidal morphology and approximately 100-nm diameter (Fig. 3), similar to the previously described exosomes.²⁰⁻²² FCM analysis demonstrated that these vesicles express exosomal markers, such as CD9, CD63, and CD81. No apparent expression of HLA-ABC and HLA-DR was observed in iPS-Exos (Fig. 4).

iPS-Exos May Help Promote the Migration of Fibroblasts Isolated from Diabetic Mice in Vitro

We analyzed iPS-Exo effects on the migration of primary cultured fibroblasts isolated from diabetic mice (Figs. 5A-5C). Compared with that of the control cells (M-Exo stimulation), fibroblasts stimulated by iPS-Exos (100 μ g/ml) showed 1.06- and 1.10-fold faster migration into the scratched areas at 12 and 24 h, respectively, after making the wound, although these differences were not statistically significant. Migration rates of diabetic mouse fibroblasts into scratched areas after 24-h incubation with 10, 50, 100, or 200 μ g/ml iPS-Exo increased with the concentration, up to 200 μ g/ml iPS-Exo concentration, where a decrease in migration rate was observed (Fig. 5B). In Figure 5C, the time course of migration of cells treated with 100 μ g/ml iPS-Exo is presented. Compared with that of the control cells (M-Exo stimulation), fibroblasts stimulated by iPS-Exos (100 μ g/ml) showed faster migration into the scratched areas at 24 h after making the wound. These differences were statistically significant (Fig. 5).

iPS-Exos Tend to Promote the Proliferation of Fibroblasts Isolated from Diabetic Mice in Vitro

Compared with that of the control, fibroblasts stimulated by iPS-Exos exhibited 1.02- and 1.09-fold increase in the proliferation rate at 48 and 72 h, respectively, following the making of wounds, but these differences were not statistically significant (Fig. 6). In Fig. 6, only the result of 48 hours is shown.

iPS-Exos Promote Cutaneous Wound Healing in Diabetic Mice

After making two wound sites in the dorsal skin of diabetic mice, we treated the wounds by PBS (untreated group), M-Exo (control group), or iPS-Exo (experimental group), and evaluated would healing rates (Fig. 7). The size of wounds treated with PBS relative to their initial size was 52.4 ± 18.8 , 30.9 ± 16.3 , 11.2 ± 3.4 , 2.0 ± 2.5 , and $0.3 \pm 0.6\%$ at day 7, 10, 14, 18, and 21, respectively. The size of wounds treated with M-Exo relative to their initial size was 41.0 ± 4.5 , 31.2 ± 6.0 , 14.1 ± 7.8 , 1.9 ± 4.1 , and $0.3 \pm 0.6\%$ at day 7, 10, 14, 18, and 21, respectively.

Exosome roles in wound healing

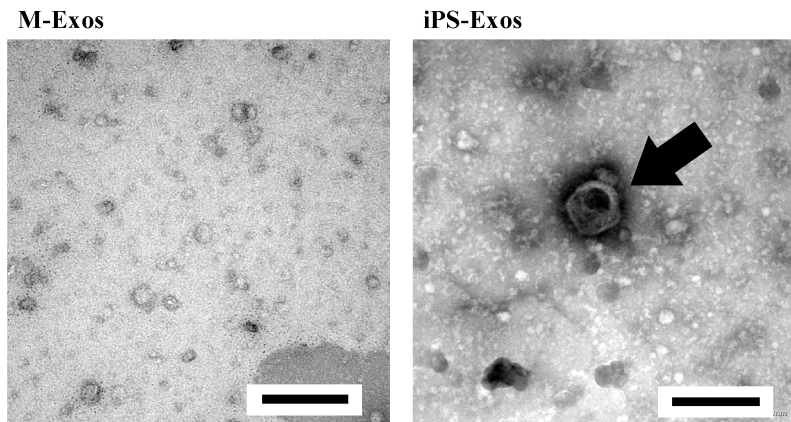


Fig. 3 Electron micrographs of induced pluripotent stem cell exosomes (iPS-Exos)
Representative images of vesicles with approximately 100-nm diameters in iPS-Exos samples, which were not observed in M-Exos (control group) samples. Scale bars, 200 nm.

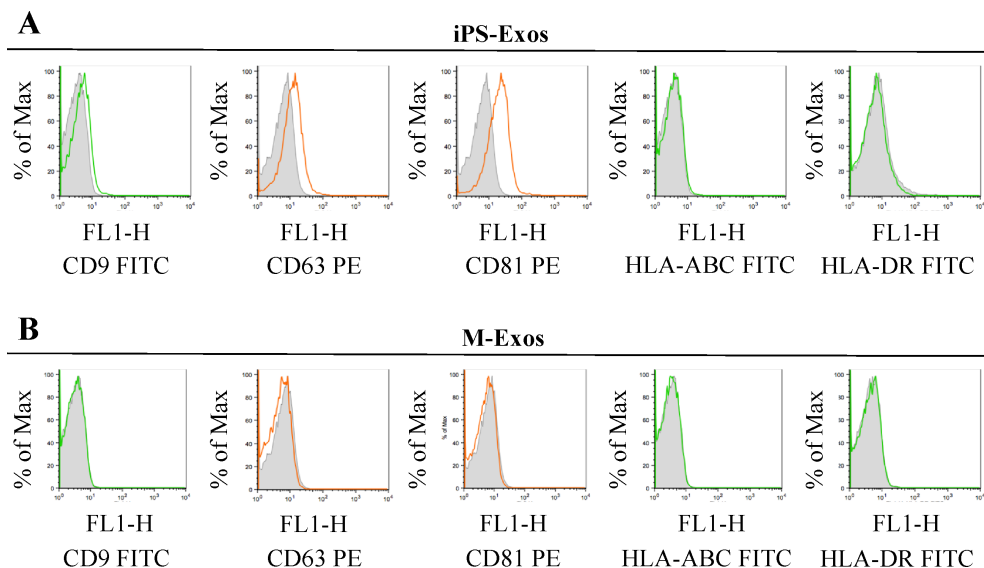
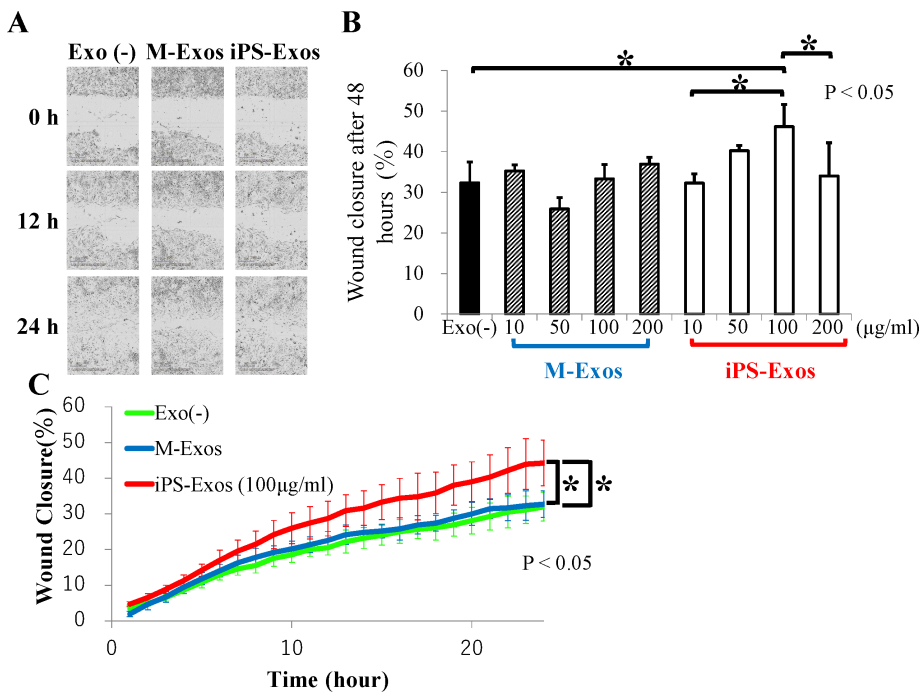


Fig. 4 Surface antigen expression on the isolated exosomes
Representative analysis showing surface expression of CD9, CD63, CD81, HLA-ABC, and HLA-DR in the induced pluripotent stem cell-derived exosomes (iPS-Exo) (A) and control sample exosomes (M-Exo) (B) coupled to aldehyde-sulfate latex beads. FITC-conjugated isotype controls and PE-conjugated isotype controls are included for comparison.

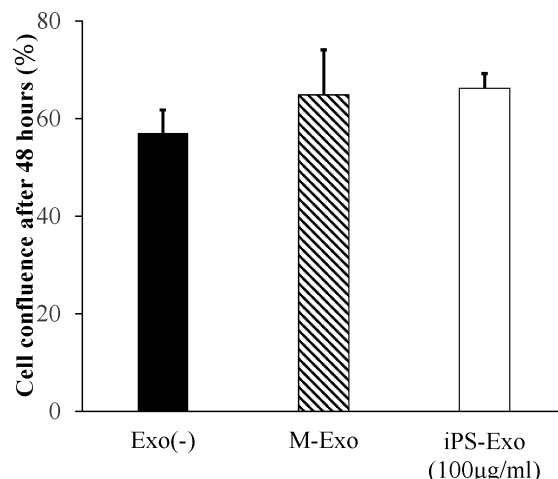
The size of wounds treated with iPS-Exos relative to their initial size was 22.3 ± 1.9 , 15.1 ± 7.8 , 10.3 ± 10.3 , 0.1 ± 0.1 , and $0.0 \pm 0.0\%$ at day 7, 10, 14, 18, and 21, respectively. Therefore, wound closure was shown to be induced in mice treated with iPS-Exos compared with that in the control and untreated groups at day 7 and 10 after inducing the wounds (Figs. 7A–7C). In iPS-Exo, M-Exo, and PBS-treated groups, complete wound closure was shown to occur after 19.0 ± 3.6 , 18.5 ± 3.3 , and 18.7 ± 2.4 days, respectively, but no statistically significant

**Fig. 5** Scratch assay results

(A) Effect of induced pluripotent stem cell-derived exosomes (iPS-Exos) on cell migration of diabetic mouse fibroblasts. Representative phase contrast images of cells migrating into wounded area at 0, 12, and 24 h in an *in vitro* scratch assay are presented. Bars, 300 μ m.

(B) Migration rates of diabetic mouse fibroblasts into scratched areas after 24-h incubation with 10, 50, 100, or 200 μ g/ml iPS-Exo.

(C) Cell migration time course. Cell migration was quantified using relative wound density (RWD). Error bars represent standard deviations (SD).

**Fig. 6** Proliferation assay results

Effect of induced pluripotent stem cell-derived exosomes (iPS-Exos) on the proliferation of diabetic mouse fibroblasts. Proliferation rates of diabetic mouse fibroblasts treated with 100 μ g/ml iPS-Exo for 48 h. Error bars, standard deviations (SD).

Exosome roles in wound healing

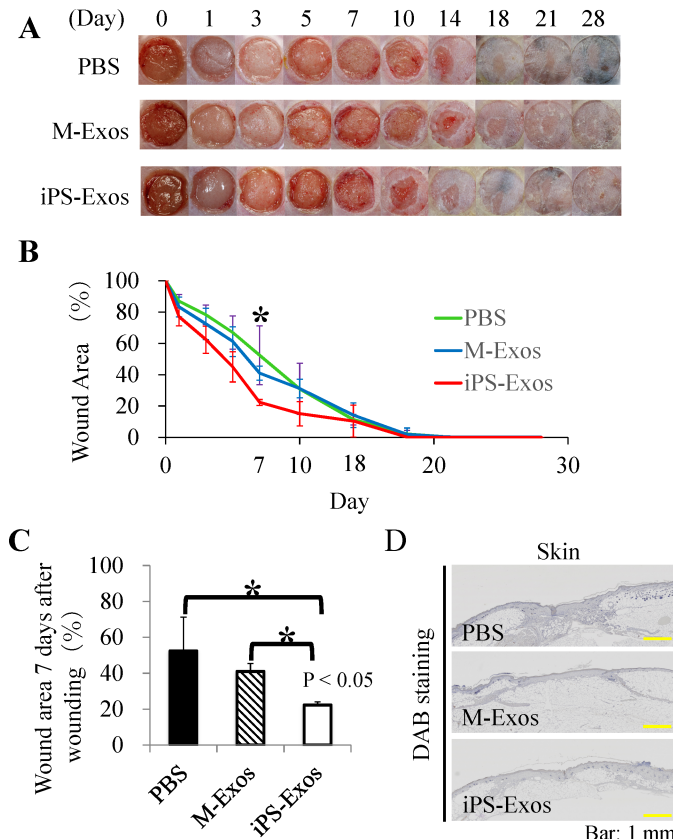


Fig. 7 Wound closure in db/db mice

- (A) Representative images of wounds treated with phosphate-buffered saline (PBS), control exosomes (M-Exos), or induced pluripotent stem cell-derived exosomes (iPS-Exos) at day 0, 1, 3, 5, 7, 10, 14, 18, 21, and 28.
- (B) Quantification of PBS, M-Exo, or iPS-Exo treatment effects at day 0, 1, 3, 5, 7, 10, 14, 18, 21, and 28. *P < 0.05, until day 7.
- (C) The rates of wound healing following different treatments. P < 0.05, compared with the controls.
- (D) Representative images of wound healing in the PBS, M-Exos, and iPS-Exos group.

differences were observed (Fig. 7B). At day 28 after inducing the wounds, the wound in the untreated group was shown to shrink and heal, whereas in the iPS-Exos group the epithelium is clearly stuck (Fig. 7D).

iPS-Exos Promote Angiogenesis in the Wounded Skin

Vascularization of newly formed tissues is an essential step in the wound-healing process. Newly formed vessels at wound sites were examined by CD31 and α -SMA double staining, and average vessel densities were determined (Fig. 8). The obtained data showed that the number of newly formed vessels increased during the healing process in all groups. The vessel density in iPS-Exo-treated group at day 7 was shown to be significantly higher than that in M-Exo- and PBS-treated groups.

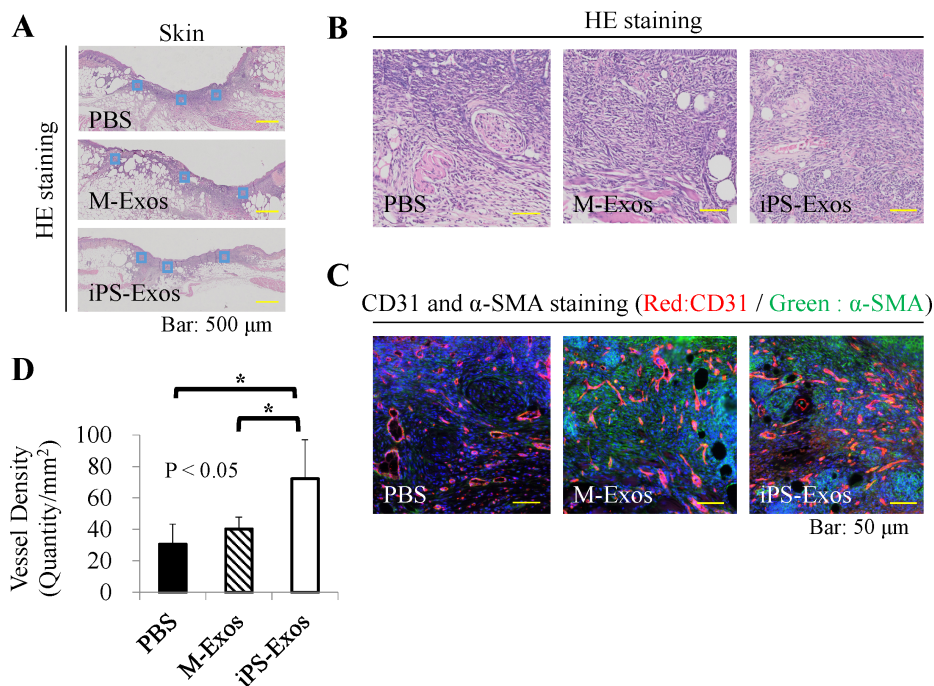


Fig. 8 Immunofluorescence analyses of vessel formation

- (A) Blood vessel numbers were determined in two areas at wound edges and three areas near the center of wounds.
- (B) Representative hematoxylin & eosin staining images.
- (C) Representative CD31 and α -SMA co-staining images, showing newly-formed vessels at wound sites.
- (D) Quantification of average vessel density in each group. * P < 0.05.

iPS-Exo Effects on the Regeneration of Peripheral Nerve Fibers

Finally, newly formed nerve fibers at wound sites were visualized and quantified by staining for neurofilament heavy polypeptide (Fig. 9). Nerve densities determined in iPS-Exo-, M-Exo-, and PBS-treated wounds at day 28 were 779.8 ± 577.5 , 491.6 ± 301.3 , and 233.4 ± 162.5 , respectively. No statistically significant difference ($P = 0.291$) was observed in nerve densities between iPS-Exo- and M-Exo-treated groups, but the nerve density in iPS-Exo-treated groups was shown to be higher than that in M-Exo-treated groups.

DISCUSSION

Previously, the potential effects of exosomes derived from mesenchymal stem cells on wound healing were studied *in vivo*.²³⁾ The *in vivo* roles of iPS-Exos, however, have not been studied extensively. Here, we demonstrated for the first time that iPS-Exos can induce wound healing in diabetic mice. Excisional wounds in diabetic mice have been reported to show significant delay in wound closure and decrease in wound bed vascularity, compared with those in the healthy mice.²⁴⁾ The results of our study showed that iPS-Exos promote wound healing in diabetic mice, suggesting the potential of iPS-Exos for the treatment of skin diseases developing in diabetic patients. Our *in vitro* experiments demonstrated that iPS-Exos tend to induce the migratory and

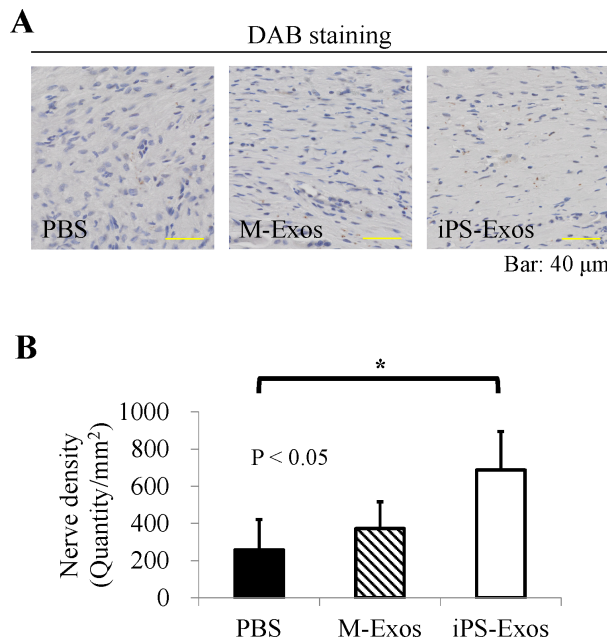


Fig. 9 Immunofluorescence analyses of neurofilaments

(A) The number of neurofilament heavy polypeptide-positive cells determined in two areas at the wound edge and in three areas near the wound center.

(B) Quantification of neurofilament heavy polypeptide expression. * P < 0.05.

proliferative capacity of diabetic mouse skin fibroblasts, suggesting that iPS-Exos exert their effects directly on the cells. Scratch assay results demonstrated that iPS-Exos induce concentration-dependent increase in the migratory potential of mouse fibroblasts, up to the concentration of 200 µg/ml iPS-Exos. This may be explained by an increase in the viscosity of the sample due to the increased concentrations of exosomes, which prevented accurate sampling. Although we did not elucidate the mechanisms of iPS-Exo-induced migration and proliferation, it is possible that cytokines or chemokines in iPS-Exos alter fibroblast phenotype. Further experiments will be needed to determine the mechanisms underlying the observed effects.

One limitation of our study was that we used M-Exo, which was prepared using only medium, as a control in all the experiments. Considering the iPS cell culturing method, involving feeder cells, the total iPS-Exos most likely involved the exosomes derived from the feeder cells as well. Future studies should attempt to discriminate the effect of iPS-derived exosomes and feeder cell-derived ones. One intriguing hypothesis is that the intercommunication between iPS cells and feeder cells through soluble factors or physical interaction leads to the production of iPS-Exo that has beneficial effects on would closure.

Murine excisional wound models have been described in many previous studies. Although animal strain, age, sex, and excisional wound size varied between these studies, the median time required for wound closure ranged from 14 to 28 days. Our *in vivo* experiments demonstrated that the early healing of wounds treated with iPS-Exos is faster than that in the control group, further indicating the potential of iPS-Exos for the development of therapeutics for the treatment of skin diseases in diabetic patients. One potential strategy that should be further examined is the continuous administration of iPS-Exos through an infusion pump. No differences in the closing

times of the wound were observed compared with those in the PBS-treated group, but iPS-Exos induced the healing of epithelium, in contrast to healing by shrinkage observed in the PBS group, confirming the potential of iPS-Exos in the treatment of skin diseases in diabetic patients.

Furthermore, we demonstrated here that iPS-Exo treatment induces the increase in the density of blood vessels on day 7 after the wounding and the increase in the density of nerve fibers on day 28 after the wounding, suggesting that these vesicles may promote the regeneration of the peripheral nervous system. Although it remains unclear whether iPS-Exos directly affect endothelial and nerve cells, the obtained data further support the potential use of iPS-Exos for skin disease treatments in diabetic patients. Additionally, iPS-Exos showed no apparent expression of HLA-ABC and -DR, suggesting the immune tolerance of these cells, and it is possible that allogeneic iPS cells may be used for future treatments.

DECLARATIONS OF INTEREST

The authors report no conflicts of interest. The authors are responsible for the content and writing of the paper.

ACKNOWLEDGEMENTS

This research was supported by the Challenging Sprouts Research Program through the Japan Society for the Promotion of Science (7115K15652). We thank Kaori Ushida (Nagoya University) for technical assistance with immunohistochemical analyses. The authors also wish to acknowledge the members of the Division for Medical Research Engineering, Nagoya University Graduate School of Medicine, for technical support with TEM, FACSCalibur, and Incucyte ZOOM-HD-2CLR.

REFERENCES

- 1) International Diabetes Federation. IDF Diabetes Atlas, (7th ed.) Brussels, Belgium: International Diabetes Federation, 2015.
- 2) Bobrie A, Colombo M, Raposo G, Thery C. Exosome secretion: molecular mechanisms and roles in immune responses. *Traffic*, 2011; 12(12): 1659–1668.
- 3) Brem H, Tomic-Canic M. Cellular and molecular basis of wound healing in diabetes. *J Clin Invest*, 2007; 117(5): 1219–1222.
- 4) Cavanagh P, Attinger C, Abbas Z, Bal A, Rojas N, Xu ZR. Cost of treating diabetic foot ulcers in five different countries. *Diabetes Metab Res Rev*, 2012; 28 Suppl 1: 107–111.
- 5) Chen L, Tredget EE, Wu PY, Wu Y. Paracrine factors of mesenchymal stem cells recruit macrophages and endothelial lineage cells and enhance wound healing. *PLoS One*, 2008; 3(4): e1886.
- 6) Cho JW, Kang MC, Lee KS. TGF-beta1-treated ADSCs-CM promotes expression of type I collagen and MMP-1, migration of human skin fibroblasts, and wound healing *in vitro* and *in vivo*. *Int J Mol Med*, 2010; 26(6): 901–906.
- 7) Fong CY, Tam K, Cheyyatraivendran S, Gan SU, Gauthaman K, Armugam A, *et al.* Human Wharton's jelly stem cells and its conditioned medium enhance healing of excisional and diabetic wounds. *J Cell Biochem*, 2014; 115(2): 290–302.
- 8) Galiano RD, Michaels J 5th, Dobryansky M, Levine JP, Gurtner GC. Quantitative and reproducible murine model of excisional wound healing. *Wound Repair Regen*, 2004; 12(4): 485–492.
- 9) Geerlings SE, Hoepelman AI. Immune dysfunction in patients with diabetes mellitus (DM). *FEMS Immunol Med Microbiol*, 1999; 26(3–4): 259–265.
- 10) Hayes NV, Blackburn E, Boyle MM, Russell GA, Frost TM, Morgan BJ, *et al.* Expression of neuregulin

- 4 splice variants in normal human tissues and prostate cancer and their effects on cell motility. *Endocr Relat Cancer*, 2010; 18(1): 39–49.
- 11) Hunt NA, Liu GT, Lavery LA. The economics of limb salvage in diabetes. *Plast Reconstr Surg*, 2011; 127 Suppl 1: 289s–295s.
 - 12) Kanitkar M, Jaiswal A, Deshpande R, Bellare J, Kale VP. Enhanced growth of endothelial precursor cells on PCG-matrix facilitates accelerated, fibrosis-free, wound healing: a diabetic mouse model. *PLoS One*, 2013; 8(7): e69960.
 - 13) Mathivanan S, Ji H, Simpson RJ. Exosomes: extracellular organelles important in intercellular communication. *J Proteomics*, 2010; 73(10): 1907–1920.
 - 14) Michaels JT, Churgin SS, Blechman KM, Greives MR, Aarabi S, Galiano RD, et al. db/db mice exhibit severe wound-healing impairments compared with other murine diabetic strains in a silicone-splinted excisional wound model. *Wound Repair Regen*, 2007; 15(5): 665–670.
 - 15) Ragnarson Tennvall G, Apelqvist J. Health-economic consequences of diabetic foot lesions. *Clin Infect Dis*, 2004; 39 Suppl 2: S132–S139.
 - 16) Santonocito M, Vento M, Guglielmino MR, Battaglia R, Wahlgren J, Ragusa M, et al. Molecular characterization of exosomes and their microRNA cargo in human follicular fluid: bioinformatic analysis reveals that exosomal microRNAs control pathways involved in follicular maturation. *Fertil Steril*, 2014; 102(6): 1751–1761.e1.
 - 17) Schorey JS, Bhatnagar S. Exosome function: from tumor immunology to pathogen biology. *Traffic*, 2008; 9(6): 871–881.
 - 18) Simpson RJ, Lim JW, Moritz RL, Mathivanan S. Exosomes: proteomic insights and diagnostic potential. *Expert Rev Proteomics*, 2009; 6(3): 267–283.
 - 19) Thery C, Amigorena S, Raposo G, Clayton A. Isolation and characterization of exosomes from cell culture supernatants and biological fluids. *Curr Protoc Cell Biol*, 2006; Chapter 3: Unit 3.22.
 - 20) Thery C, Zitvogel L, Amigorena S. Exosomes: composition, biogenesis and function. *Nat Rev Immunol*, 2002; 2(8): 569–579.
 - 21) van Niel G, Porto-Carreiro I, Simoes S, Raposo G. Exosomes: a common pathway for a specialized function. *J Biochem*, 2006; 140(1): 13–21.
 - 22) Wahlgren J, De LKT, Brisslert M, Vaziri Sani F, Telemo E, Sunnerhagen P, et al. Plasma exosomes can deliver exogenous short interfering RNA to monocytes and lymphocytes. *Nucleic Acids Res*, 2012; 40(17): e130.
 - 23) Yoshioka Y, Konishi Y, Kosaka N, Katsuda T, Kato T, Ochiya T. Comparative marker analysis of extracellular vesicles in different human cancer types. *J Extracell Vesicles*, 2013; 2.
 - 24) Zhang J, Guan J, Niu X, Hu G, Guo S, Li Q, et al. Exosomes released from human induced pluripotent stem cells-derived MSCs facilitate cutaneous wound healing by promoting collagen synthesis and angiogenesis. *J Transl Med*, 2015; 13: 49.